

2015

## Path integrals, matter waves, and the double slit

Eric R. Jones

*University of Nebraska-Lincoln*, [eric.ryan.jones@huskers.unl.edu](mailto:eric.ryan.jones@huskers.unl.edu)

Roger Bach

*University of Nebraska-Lincoln*, [roger.bach@gmail.com](mailto:roger.bach@gmail.com)

Herman Batelaan

*University of Nebraska-Lincoln*, [hbatelaan@unl.edu](mailto:hbatelaan@unl.edu)

Follow this and additional works at: <http://digitalcommons.unl.edu/physicsbatelaan>

---

Jones, Eric R.; Bach, Roger; and Batelaan, Herman, "Path integrals, matter waves, and the double slit" (2015). *Herman Batelaan Publications*. 2.

<http://digitalcommons.unl.edu/physicsbatelaan/2>

This Article is brought to you for free and open access by the Research Papers in Physics and Astronomy at DigitalCommons@University of Nebraska - Lincoln. It has been accepted for inclusion in Herman Batelaan Publications by an authorized administrator of DigitalCommons@University of Nebraska - Lincoln.

# Path integrals, matter waves, and the double slit

Eric R Jones, Roger A Bach and Herman Batelaan

Department of Physics and Astronomy, University of Nebraska–Lincoln, Theodore P. Jorgensen Hall, Lincoln, NE 68588, USA

E-mail: [eric.ryan.jones@huskers.unl.edu](mailto:eric.ryan.jones@huskers.unl.edu) and [hbatelaan2@unl.edu](mailto:hbatelaan2@unl.edu)

Received 16 June 2015, revised 8 September 2015

Accepted for publication 11 September 2015

Published 13 October 2015



CrossMark

## Abstract

Basic explanations of the double slit diffraction phenomenon include a description of waves that emanate from two slits and interfere. The locations of the interference minima and maxima are determined by the phase difference of the waves. An optical wave, which has a wavelength  $\lambda$  and propagates a distance  $L$ , accumulates a phase of  $2\pi L/\lambda$ . A matter wave, also having wavelength  $\lambda$  that propagates the same distance  $L$ , accumulates a phase of  $\pi L/\lambda$ , which is a factor of two different from the optical case. Nevertheless, in most situations, the phase difference,  $\Delta\varphi$ , for interfering matter waves that propagate distances that differ by  $\Delta L$ , is approximately  $2\pi\Delta L/\lambda$ , which is the same value computed in the optical case. The difference between the matter and optical case hinders conceptual explanations of diffraction from two slits based on the matter–optics analogy. In the following article we provide a path integral description for matter waves with a focus on conceptual explanation. A thought experiment is provided to illustrate the validity range of the approximation  $\Delta\varphi \approx 2\pi\Delta L/\lambda$ .

Keywords: quantum mechanics, path integrals, double slit, matter optics

(Some figures may appear in colour only in the online journal)

## 1. Introduction

The presentation of the double slit typically begins with a discussion of Young's original experiments [1] on the diffraction and interference of light. Demonstrations such as a ripple tank, one of Young's own inventions [2], are used to reinforce the concept of wave interference and Huygens' principle of the superposition of waves [3]. Figure 1 shows circular waves that impinge on a pair of narrow slits having separation  $d$ . The slits become themselves

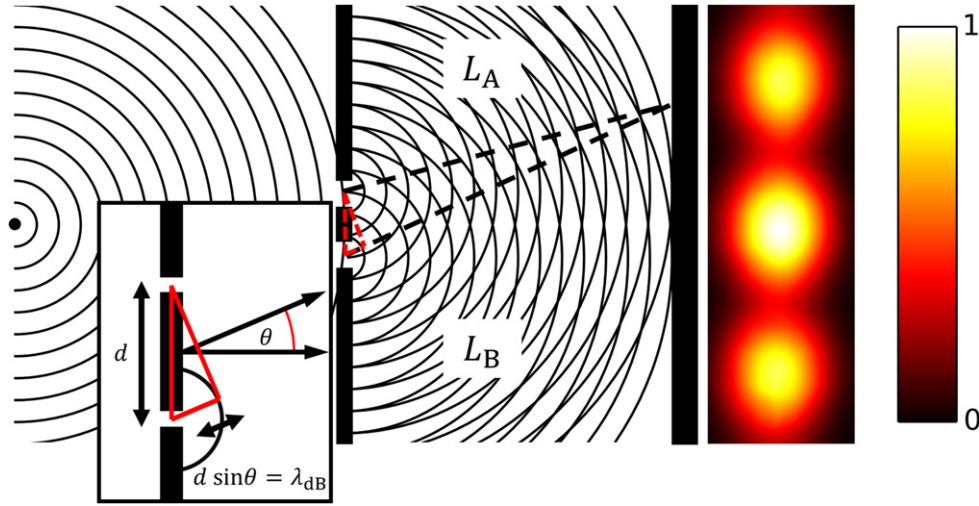


**Figure 1.** Typical schematic of Young's two-slit arrangement. The condition for first order constructive interference,  $d \sin(\theta) = \lambda$ , is illustrated. Shown right is recently published data for an electron double slit interference experiment [4].

new sources of circular waves. The phase associated with a wave is the number of wavefronts counted along a line with length  $L$ , that is,  $L/\lambda$ , multiplied by  $2\pi$ . Waves interfere constructively when the phase difference is an integer multiple of  $2\pi$ . These ideas lead to the familiar condition for constructive interference

$$\Delta L = d \sin(\theta) = n\lambda, \quad (1)$$

where  $n$  indicates the diffraction order that occurs at the diffraction angle  $\theta$ . This analysis represented in figure 1, where a phase  $2\pi L/\lambda$  is prescribed to a path of length  $L$ , describes what we will hereby refer to as the 'optical analogy.' Even though this approach is correct for light, it is not for matter. The first problem is that it uses an incorrect phase,  $2\pi L/\lambda_{dB}$ , for a matter wave (where  $\lambda_{dB}$  is the de Broglie wavelength). The second problem is that the use of the optical analogy will nevertheless give the correct phase difference for most situations.

In this article, the optical analogy and its limits of validity are discussed for matter waves. The analogy is also compared to a stationary phase method motivated by the path integral formalism. The path integral formalism is shown in section 2 to give a single path phase of  $\pi L/\lambda_{dB}$ , and a phase difference between two interfering paths that is approximately  $2\pi\Delta L/\lambda_{dB}$ . The phase difference in optics,  $2\pi\Delta L/\lambda$ , is the same. The space-time formulation of the path integral formalism [5] describes paths starting and ending at fixed positions, of varying length, over a fixed time interval for interfering paths. Therefore, the path integral formalism assigns different speeds (and thus wavelengths) to such different paths. This appears to be inconsistent with the idea that a double slit is illuminated with a wave described by one speed or wavelength. This apparent inconsistency will be clarified in the next sections. In sections 3–5, the relation to the optical case, wave mechanics, and time-dependence is discussed, respectively, and it is demonstrated that the optical case is fundamentally different from the matter case, despite their similarities. Section 6 discusses how the uncertainty principle relates to the path integral results. In sections 7 through 11, a stationary phase argument completes the justification for the path selections made in section 2. At this point, it may appear that apart from some conceptual details, the optical analogy's validity can

be justified by the path integral method. In section 12, a thought experiment is discussed for which the optical analogy predicts phase differences that disagree with the path integral method, with the purpose to illustrate that the optical analogy agrees only approximatively.

## 2. Determining the phase from the path integral

Feynman developed a method [5] to construct solutions to Schrödinger's equation [6] based on Dirac's observations on the relationship between the evolution of quantum states between points in space–time and the classical notion of particle trajectories [7]. In Feynman's path integral formalism, a probability amplitude is determined from a phase,  $\varphi_{\text{path}}$ , computed along a particular path connecting two space–time events. The total probability amplitude  $K(\beta; \alpha)$  for finding a particle at location  $x_\beta$  at time  $t_\beta$ , having started at location  $x_\alpha$  at the earlier time  $t_\alpha$ , is given by the sum

$$K(\beta; \alpha) = \sum_{\text{all paths } \alpha \rightarrow \beta} \text{const} \cdot \exp(i\varphi_{\text{path}}), \quad (2)$$

where all paths connect events  $\alpha$  and  $\beta$  [8]. The phase  $\varphi_{\text{path}}$  accumulated along any path is given by

$$\varphi_{\text{path}} = \frac{1}{\hbar} \int_{\text{path}} L(x, \dot{x}, t) dt, \quad (3)$$

where  $L$  is the Lagrangian function, which depends on the positions,  $x$ , speeds,  $\dot{x}$ , and times,  $t$ , along the path. This path integral method is used to efficiently describe experimental results for matter interferometry [9], for example the double slit experiment for electrons (see the supplementary material of [4], available online).

For the case of a particle moving in free space in 1D, the Lagrangian is

$$L(x, \dot{x}, t) = \frac{m}{2} \dot{x}^2. \quad (4)$$

In free space, the path integral accumulated phase,

$$\varphi_{\text{path}} = \frac{m}{2\hbar} \left( \frac{x_\beta - x_\alpha}{t_\beta - t_\alpha} \right)^2 (t_\beta - t_\alpha) = \frac{m}{2\hbar} \frac{(x_\beta - x_\alpha)^2}{t_\beta - t_\alpha}, \quad (5)$$

is a function of the endpoints only. Consider  $x_\alpha = 0$  and  $x_\beta = x$ , with  $t_\alpha = 0$  and  $t_\beta = t$  as a fixed time. When  $\varphi_{\text{path}} \gg 2\pi$ , the distance between points in space where the phase varies by  $2\pi$  approaches a constant value  $\lambda$ , determined from (5) by

$$2\pi = \frac{m}{2\hbar} \frac{(x + \lambda)^2}{t} - \frac{m}{2\hbar} \frac{x^2}{t} \cong \frac{m}{2\hbar} \frac{2x\lambda}{t}, \quad (6)$$

where it is assumed  $x \gg \lambda$ . The value of  $\lambda$  follows from (6) as  $\lambda = \hbar t/mx$ , or in terms of the average speed  $v = x/t$  as  $\lambda = \hbar/mv$ . In free space, the classical momentum is  $p = mv$ , so  $\lambda$  can be identified with the de Broglie wavelength defined  $\lambda_{\text{dB}} \equiv \hbar/p$ . By substituting  $x_\beta - x_\alpha = L$  and the above definitions into (5), the path integral accumulated phase is thus

$$\varphi_{\text{path}} = \frac{\pi L}{\lambda_{\text{dB}}}, \quad (7)$$

which followed from the discussion above taken from Feynman and Hibbs [8] (in particular, (3.7)–(3.10)).

Now consider a double slit illuminated with a matter wave that is characterized by one speed. This system can be qualitatively described by the interference of two paths, represented by the dashed lines of figure 1. A reasonable assumption would be that the speed, and thus the de Broglie wavelength, is the same for both paths, so the phase difference  $\Delta\varphi$  for paths of lengths  $L_A$  and  $L_B$  from (7) is

$$\Delta\varphi = \varphi_B - \varphi_A = \frac{\pi}{\lambda_{dB}}(L_B - L_A). \quad (8)$$

This result is incompatible with the phase difference obtained from the optical analogy because it differs by a factor of 2. This result is also incompatible with experiment, which agrees with the optical analogy. This is fine because it is indeed incorrect; the false assumption made is that the speeds along both paths are the same. Even though this result may appear quite surprising at first, the presence of a distribution of momenta, and hence multiple speeds, is familiar in the description of wave packets (see section 4). The correct result according the path integral formalism can only be recovered by noting that interfering paths have equal durations  $\Delta t$  in time; they both must begin at  $\alpha$  and end at  $\beta$ , as expressed in (2). Because  $L_A$  and  $L_B$  are not equal, the consequence is that paths A and B have different speeds. The corresponding de Broglie wavelengths for paths A and B are then

$$\lambda_{A,B} = \frac{h\Delta t}{mL_{A,B}}. \quad (9)$$

The path length difference  $\delta L$  between the two paths is taken to be small in comparison to the path lengths  $L_{A,B}$ . For  $L_A < L_B$ , the de Broglie wavelength can be expanded as

$$\lambda_B \cong \frac{h\Delta t}{mL_A} \left\{ 1 - \frac{\delta L}{L_A} + O\left[\left(\frac{\delta L}{L_A}\right)^2\right] \right\} \cong \lambda_A \left( 1 - \frac{\delta L}{L_A} \right). \quad (10)$$

Terms of order  $O[(\delta L/L_A)^2]$  are neglected. The phase difference between the two paths is

$$\Delta\varphi = \varphi_B - \varphi_A \cong \frac{\pi L_B}{\lambda_A \left( 1 - \frac{\delta L}{L_A} \right)} - \frac{\pi L_A}{\lambda_A} \cong \frac{2\pi(L_B - L_A)}{\lambda_A}. \quad (11)$$

Thus, the correct result is recovered and justified by the path integral formalism of quantum mechanics. These results can be applied in an undergraduate course utilizing the level of description indicated in (1).

### 3. Comparison to the optical case

The question may arise why the analogous situation of two slit diffraction for light presents no conceptual difficulty. The use of straight paths in figure 1 for light could be justified by the application of Fermat's principle of least time [10]. These paths are called rays in the geometrical optics formulation of light propagation [11–13]. Rays are constructed from the normals of a succession of electromagnetic wave-fronts. Each ray is associated with a phase called the eikonal  $\phi$  that is calculated in a homogeneous medium as

$$\phi = \int_{\text{ray}} k \cdot dl = \int_{\text{ray}} \omega dt. \quad (12)$$

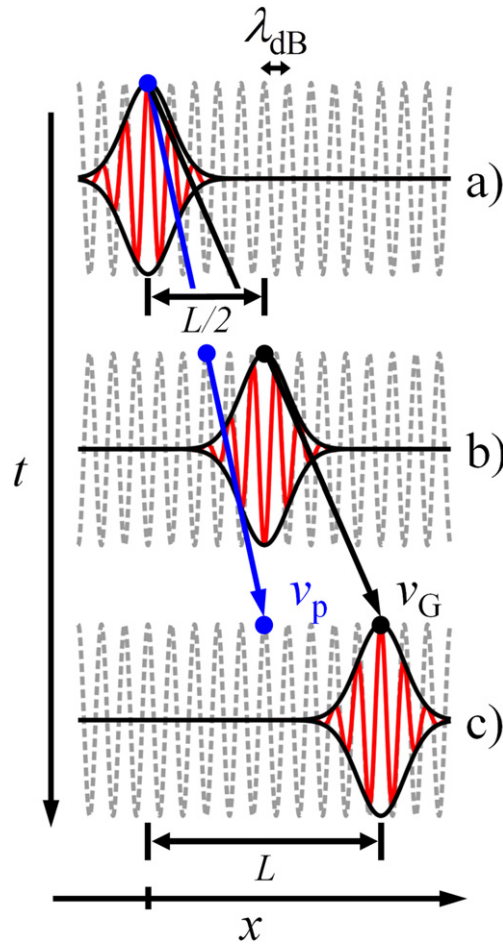


**Figure 2.** Matter wave propagation. Three snapshots in time of the evolution of a Gaussian wave packet are shown in (a)–(c). A point on the carrier wave, shown as a blue dot, moves to the right at the phase velocity  $v_p$ , indicated with the blue line. The centre of the envelope, which is synchronous with the blue dot at (a), moves at the group velocity  $v_G = 2v_p$ , indicated with the black line. A pulse that propagates a length  $L$  accumulates a phase  $\varphi = kL - \omega t$ . The angular frequency is given by  $\omega = kv_p$ , while the propagation time is given by  $t = L/v_G$ . Substitution gives that  $\varphi = \pi L/\lambda_{dB}$ , which differs from the optical analogy of counting waves along the distance multiplied by  $2\pi$ , indicated by the blue dot in (c).

For light, this phase has the value  $\int \mathbf{k} \cdot d\mathbf{l} = kL = 2\pi L/\lambda$  along a ray. This justifies the optical analogy of counting wave-fronts along the propagation paths as in the still pictures of figure 1. The equality of the two integrals in (12) implies (note  $dl/dt = c$ ) that the dispersion relation for light is linear:

$$\omega = |k| c. \quad (13)$$

The dispersion relation determines the group and phase velocities. For light propagating in free space, these velocities are the same. Matter wave propagation is different from light because it has a quadratic dispersion relation [14] and the group and phase velocities are not

the same. The connection between speed and phase for matter waves is discussed in the following section.

#### 4. Determining the phase from the wave description: the motion picture

Consider the motion of a one dimensional electron wave packet, illustrated in figure 2. This superposition of waves  $\psi(x, t)$  is given by the Fourier transform of the momentum distribution  $f(k - k_0)$  of the constituent waves in the group:

$$\psi(x, t) = \int_{-\infty}^{\infty} f(k - k_0) \exp(i[kx - \omega(k)t]) dk. \quad (14)$$

For a Gaussian momentum distribution  $f(k - k_0) = \exp[-(k - k_0)^2/2(\Delta k)^2]$  with width  $\Delta k$  and a dispersion relation  $\omega(k) = \hbar k^2/2m$ , the wave packet  $\psi(x, t)$  is then approximately given by

$$\begin{aligned} \psi(x, t) &\propto \exp(i[kx - \omega(k)t]) \exp\left[-\frac{(\Delta k)^2}{2}\left(x - \frac{\hbar k_0}{m}t\right)^2\right] \\ &= \exp\left[ik_0\left(x - \frac{\hbar k_0}{2m}t\right)\right] \exp\left[-\frac{(\Delta k)^2}{2}\left(x - \frac{\hbar k_0}{m}t\right)^2\right]. \end{aligned} \quad (15)$$

A typical matter wave packet's width spreads and its frequency components disperse as time evolves; however, for sufficiently short times this spreading and dispersion can be neglected. The real part of (15) is illustrated in figure 2 for three times [15, 16]. The first exponential factor, represented by a dashed grey line in figure 2, is a sinusoidal carrier wave travelling with the phase velocity

$$v_P \equiv \frac{\omega(k)}{k} \Big|_{k=k_0} = \frac{\hbar k_0}{2m}. \quad (16)$$

The second factor is the Gaussian envelope, represented by a solid black line, whose centre (black dots) travels twice as fast as the sinusoidal wave at the group velocity

$$v_G \equiv \frac{\partial \omega(k)}{\partial k} \Big|_{k=k_0} = \frac{\hbar k_0}{m} = 2v_P. \quad (17)$$

The group velocity is identified with the particle speed and determines the de Broglie wavelength. Suppose that the wave packet in figure 2 travels a distance  $L$  in a time  $\Delta t$ . The connection between  $L$  and  $\Delta t$  is determined by the motion of the centre of the Gaussian envelope as

$$L = \frac{\hbar k_0}{m} \Delta t. \quad (18)$$

Substituting this relationship into the phase argument of the carrier wave in (15) gives an accumulated phase  $\varphi$  of

$$\varphi = \frac{k_0 L}{2} = \frac{\pi L}{\lambda_0}. \quad (19)$$

Thus the phase accumulated by a matter wave packet moving from one position to another follows from inspecting a time-dependent solution, and not from the time-independent part alone. Note that this result agrees with the single path accumulated phase derived in (7), but it cannot lead to the correct phase difference between two paths (11) because only one group

velocity is present. The results in this section could be discussed in an introductory course in modern physics or undergraduate courses in quantum mechanics.

## 5. The time-independent and time-dependent Schrödinger equations

The fact that none of the experimental parts of a double slit experiment changes over time suggests inspecting a steady state solution. Consider the time-dependent Schrödinger equation,

$$-\frac{\hbar^2}{2m}\nabla^2\psi - V\psi = i\hbar\frac{\partial\psi}{\partial t}. \quad (20)$$

When the potential  $V$  in the Schrödinger equation does not depend on time, then the time-independent equation is derived from the time-dependent equation by separation of variables and division by the common factor  $\exp(-i\omega t)$ . This results in the time-independent Schrödinger equation,

$$\nabla^2\varphi + \frac{2(E - V)}{m\hbar^2}\varphi = 0. \quad (21)$$

The factor  $2(E - V)/m\hbar^2$  can be defined as  $k^2$  to give the Helmholtz equation,

$$\nabla^2\varphi + k^2\varphi = 0, \quad (22)$$

the solutions of which also describe the steady state solutions for optics. This well-known analogy is a defining property of the field of matter–optics (see section 2.1 of [14]).

Solutions to the Helmholtz equation with the same energy values (and thus  $k$ -values for free space solutions) can be summed to construct a new solution, and thus the superposition principle holds. The solutions in the case illustrated in figure 1 have the simple form  $\varphi(r) = C \exp(ikr)/r$ . The circles in figure 1 can then be thought of as depicting the wave fronts of the real part of the circular waves  $\varphi_A(r_A)$  and  $\varphi_B(r_B)$  that are the solutions to the Helmholtz equation. The probability to find a particle at a position  $x$  on the detection screen is then given by the Born rule,  $|\psi(x, t)|^2 = |\varphi_A[r_A(x)] + \varphi_B[r_B(x)]|^2$ . The result is time-independent because the time-dependent factor  $\exp -i\omega t$  was factored out of the wave function. Using the lengths  $r_{A,B} = L_{A,B} = n_{A,B}\lambda_{dB}$  for each dashed straight line in figure 1 leads immediately to the condition  $\Delta L = n\lambda$  at maxima in the probability distribution.

It is then reasonable to question why the optical analogy is not sufficient to return to a time-dependent description of the double slit experiment for matter. After all, it appears that we could recover the time-dependent description by multiplying the stationary solutions  $\varphi_A$  and  $\varphi_B$  with the factor  $\exp(-i\omega t)$ . Let us associate with the waves, for a fixed energy  $E$ , the kinematic speed as given by  $v = \sqrt{2E/m}$ . The propagation time  $t$  along any direction is then  $t = r/v$ . This leads to the phase  $kr - \omega t = kr/2$  evolving from either slit to the detection screen, as in (18), when the factor  $\exp(-i\omega t)$  is added back to the wavefunction. The phase difference at a detection point would then be  $(kr_B - kr_A)/2 = \pi(r_B - r_A)/\lambda_{dB}$ , as in (8), which is incorrect. The correct use of time-dependent formalisms avoids this discrepancy, as shown in section 2.

It is also reasonable to attack the argument above as being too simplistic. After all, the full solution of the Helmholtz equation in the diffraction problem involves Green's functions for the problem [17], and Green's functions at one energy for both light and matter are the same, as they solve the same Helmholtz equation. This would give the correct spatial patterns for matter and light, and the full time-dependent results could be obtained via Fourier transform. However, the time-dependent results would still not be generally correct for matter. Because matter waves are

dispersive in free space, they experience the phenomenon of diffraction in time at a slit [18–20]. This effect, which has been realized experimentally [21, 22], requires careful consideration of Green’s function for the time-dependent Schrödinger equation. Diffraction in time changes the time-dependence of the resulting probability distribution. On the other hand, light is not dispersive in free space, so ‘there is no diffraction in time for light [19].’ Essential for our discussion is that we confirm that the spatial dependence of diffraction also changes for certain stationary configurations (see (57) of [20]). We give a simulation of an experimental configuration where these differences can be distinguished in section 12. The results of this section could be discussed in an advanced course in quantum mechanics, when students have had prior experience with partial differential equations.

## 6. The Heisenberg uncertainty principle and path measurements

It has been established from section 2 that if both paths from the slits to the screen have the same duration in time, the speeds associated with the two interfering paths will be different. These different speeds give rise to slightly different kinetic energies. Is it then possible that the actual path a particle travelled could be determined by performing an energy measurement at a particular point on the detection screen? If this would be possible, and a diffraction pattern would be present, then this would be a which-way detector and violate quantum mechanics. In the following, it is shown that this is not possible, as it violates Heisenberg’s uncertainty principle. As usual, the uncertainty relation protects quantum mechanics.

In order for interference to occur, the wave-fronts associated with the particles must arrive coherently at the detection screen. Thus, waves leading to interference at the point of detection can experience a variation in phase difference of no more than  $\pi$ ; otherwise, the interference contrast averages out. Representing the variation in phase difference as  $\delta\phi$ , the condition for interference is then

$$|\delta\phi| \lesssim \pi. \quad (23)$$

The path integral phase difference is defined from (5) as

$$\phi = \frac{1}{\hbar} \left( \frac{mL_B^2}{2\tau} - \frac{mL_A^2}{2\tau} \right), \quad (24)$$

where  $\tau = t_\beta - t_\alpha$ . The variation of phase difference  $\delta\phi$  related to a first-order variation of the time  $\tau$  is given by

$$\delta\phi = \frac{\partial\phi}{\partial\tau} \delta\tau = -\frac{1}{\hbar} \left( \frac{mL_B^2}{2\tau^2} - \frac{mL_A^2}{2\tau^2} \right) \delta\tau. \quad (25)$$

The quantity in parentheses is the difference in kinetic energy of the paths, defined as  $\Delta E$ . The condition for interference (23) leads to the inequality

$$\Delta E \delta\tau \lesssim \frac{\hbar}{2}. \quad (26)$$

The energy resolution necessary to distinguish which path a particle takes on its way from the slits to the detection point must be smaller than the kinetic energy difference  $\Delta E$  between the two interfering paths. The necessary timing resolution on the energy measurement according to (26) would thus violate the Heisenberg uncertainty principle. Therefore, preserving phase coherence protects the inability to distinguish through which slit a particle will pass on its way

to the detection point. A similar argument can be made for paths defined by fixed energy and varying arrival times.

The preceding argument for the preservation of phase coherence for energy and time measurements can also be expressed in terms of momentum and position. The condition for interference is again given by (23). The variation of the phase difference  $\delta\phi$  is determined by the variation in the measurement of the momentum  $\delta p$  as

$$\delta\phi = \frac{\partial\phi}{\partial p}\delta p, \quad (27)$$

or, in terms of the de Broglie wavelength,  $p = h/\lambda$ , and the phase difference (11),

$$\delta\phi = \frac{\partial\phi}{\partial\lambda_{\text{dB}}}\delta\lambda_{\text{dB}} = -\frac{2\pi\Delta L}{\lambda_{\text{dB}}^2}\delta\lambda_{\text{dB}}, \quad (28)$$

where  $\lambda_{\text{dB}} = \lambda_A$ . The variation in the momentum  $p$  is related to a variation in the wavelength as

$$\delta p = -\frac{h\delta\lambda_{\text{dB}}}{\lambda_{\text{dB}}^2}. \quad (29)$$

Substituting (28) and (29) into (23) gives the inequality

$$\Delta L\delta p \lesssim \frac{h}{2}. \quad (30)$$

The length resolution necessary to distinguish which path a particle takes on its way from the slits to the detection point must be smaller than the length difference  $\Delta L$  between the two interfering paths. The necessary momentum resolution on the length measurement according to (26) would thus violate the Heisenberg uncertainty principle. Therefore, a which-way measurement, that also maintains a diffraction pattern, is not possible. The level of argument presented here is appropriate in any undergraduate course presented with the Heisenberg uncertainty principle.

## 7. Revisiting the path integral propagator in free space

In section 2, we restricted the discussion of path integral phase differences in a qualitative description of the double slit to a particular selection of two paths. However, the full path integral description for the double slit calls for a summation of probability amplitudes over *all* possible paths in space and time between fixed events, not just the particular selection. In the following, section 7, we briefly review the free-space 1D propagator in the path integral formalism. In section 8, the free-space propagator is applied to the two-step event of crossing a slit at one particular time. In section 9, the sum over all slit crossing times is shown to converge to the choice of a particular time for each path in space. In section 10, the particular choice of time for each slit-crossing path is motivated by a stationary phase argument. In section 11, the stationary phase argument is illustrated in the two-path description of the double slit, as in figure 1. In section 12, the results from the stationary phase argument and a path integral sum over times are compared to the optical analogy in a near-field arrangement where paths are summed over the entire extent of the slits.

The probability amplitude for a particle to travel in free space from space-time event  $\alpha$ , denoted  $(x_0, t_0)$ , to event  $\beta$ , denoted  $(x_N, t_N)$ , in a number  $N$  evenly spaced time intervals  $\epsilon$ , is given in (3.2) of [8] as

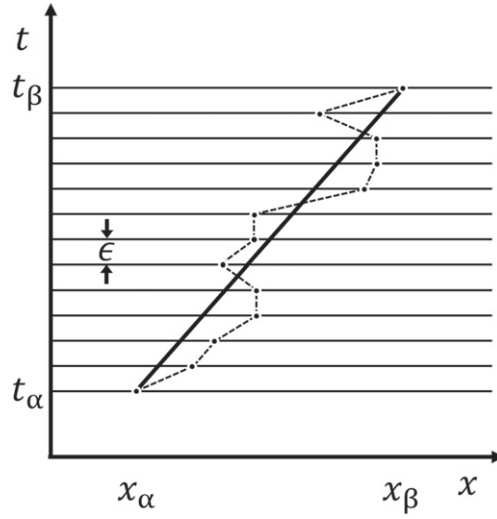


**Figure 3.** Feynman paths for 1D free particle propagation. A general path (dotted line) is shown for a point particle that travels from space–time point  $(x_\alpha, t_\alpha)$  to  $(x_\beta, t_\beta)$ . The locations  $x$  that the path crosses (indicated for times separated by  $\epsilon$ ) can be varied along the  $x$ -axis. The classical path is indicated with the bold dark line. Feynman showed that the total amplitude for motion from  $\alpha$  to  $\beta$  summed over all paths (by integrating over the  $x$ -locations) is identical to the amplitude computed along the classical path alone, which is a central result from the path integral formalism [5, 8].

$$K(\beta; \alpha) = \lim_{\epsilon \rightarrow 0} \left( \frac{m}{2\pi i \hbar \epsilon} \right)^{N/2} \int \dots \int \exp \left[ \frac{im}{2\hbar \epsilon} \sum_{j=1}^N (x_j - x_{j-1})^2 \right] dx_1 \dots dx_{N-1}. \quad (31)$$

Feynman points out that the resulting nested Gaussian integrals can be performed iteratively, leading to the result

$$K(\beta; \alpha) = \left( \frac{m}{2\pi i \hbar \cdot N\epsilon} \right)^{1/2} \exp \left[ \frac{im}{2\hbar \cdot N\epsilon} (x_N - x_0)^2 \right]. \quad (32)$$

When the subscripts 0 and  $N$  are associated with their space–time events  $\alpha$  and  $\beta$ , and the total time  $N\epsilon$  is replaced with the time difference,  $t_\beta - t_\alpha$ , then (32) becomes

$$K(\beta; \alpha) = \left[ \frac{m}{2\pi i \hbar \cdot (t_\beta - t_\alpha)} \right]^{1/2} \exp \left[ \frac{im}{2\hbar \cdot (t_\beta - t_\alpha)} (x_\beta - x_\alpha)^2 \right]. \quad (33)$$

This result, which is readily generalized to higher dimensions, shows that the amplitude associated with the summation over all possible paths connecting two events in free space is equal to the amplitude associated with the classical path alone, as sketched in figure 3. The formal path integral discussion of this section is suitable for graduate coursework in quantum mechanics.

## 8. Two-step propagator for a slit

As the next step towards describing the double slit, consider the amplitude for an electron path intersecting a single slit. This path is described by three space–time events, labelled as

follows: the source, defined as the event  $\alpha$ ; the slit crossing, denoted by slit; and the measurement at the screen,  $\beta$ .

The amplitude for such a path can be constructed as the product of the amplitude for two steps. The first step is to reach the slit from  $\alpha$ , and the second step is to travel from the slit to  $\beta$  [23, 24]. Applying the result of (33) to this case, one obtains

$$\begin{aligned}
 K(\beta; \alpha) &= K(\beta; \text{slit}) \cdot K(\text{slit}; \alpha) \\
 &= \left[ \frac{m}{2\pi i \hbar \cdot (t_\beta - t_{\text{slit}})} \right]^{1/2} \exp \left[ \frac{im}{2\hbar \cdot (t_\beta - t_{\text{slit}})} (x_\beta - x_{\text{slit}})^2 \right] \\
 &\quad \cdot \left[ \frac{m}{2\pi i \hbar \cdot (t_{\text{slit}} - t_\alpha)} \right]^{1/2} \exp \left[ \frac{im}{2\hbar \cdot (t_{\text{slit}} - t_\alpha)} (x_{\text{slit}} - x_\alpha)^2 \right] \\
 &= \frac{m}{2\pi i \hbar} \cdot \left[ \frac{1}{(t_\beta - t_{\text{slit}}) \cdot (t_{\text{slit}} - t_\alpha)} \right]^{1/2} \cdot \exp \left[ \frac{imL^2 \cdot (t_\beta - t_\alpha)}{2\hbar \cdot (t_\beta - t_{\text{slit}}) \cdot (t_{\text{slit}} - t_\alpha)} \right], \quad (34)
 \end{aligned}$$

where the substitution  $(x_\beta - x_\alpha)/2 = L$  was made. We note that this is an approximation: an exact construction for the propagator would take into account the boundary conditions set by the walls. The integrations from  $-\infty$  to  $\infty$  in (31) include paths that pass through the walls; therefore, the propagator in (34) adds extraneous paths to the sum. The times  $t_\alpha$  and  $t_\beta$  defining the boundaries of this path are fixed, but the slit-crossing time,  $t_{\text{slit}}$ , is not. It is not a measured event in the same sense as  $\alpha$  or  $\beta$  and thus cannot be specified. The total amplitude to cross the slit,  $K(\beta; \alpha)$ , is then a sum over all of the amplitudes having every possible value of  $t_{\text{slit}}$  [20].

## 9. Time summed amplitude for two-step propagator

To obtain the total amplitude to cross the slit,  $K(\beta; \alpha)$ , consider the sum of the products  $K(\beta; \text{slit}) \cdot K(\text{slit}; \alpha)$  of (34) for every value of  $t_{\text{slit}}$  occurring between  $t_\alpha$  and  $t_\beta$ . The result is written as

$$K(\beta; \alpha) = \sum_{t_{\text{slit}}=t_\alpha}^{t_\beta} K(x_\beta, t_\beta; x_{\text{slit}}, t_{\text{slit}}) \cdot K(x_{\text{slit}}, t_{\text{slit}}; x_\alpha, t_\alpha). \quad (35)$$

For more detail, see the derivation of (35) in appendix A. This formally establishes the sum over intermediate times that is required from the sum over all paths given in (31). The sum in (35) over the continuous value  $t_{\text{slit}}$  is proportional to the integral  $I(\beta; \alpha)$ , given by

$$I(\beta; \alpha) = \int_{-\frac{t_\beta}{2}}^{\frac{t_\beta}{2}} dt \frac{m}{2\pi i \hbar} \left[ \frac{1}{\left(\frac{t_\beta}{2} - t\right) \cdot \left(\frac{t_\beta}{2} + t\right)} \right]^{1/2} \exp \left[ \frac{imL^2 \cdot t_\beta}{2\hbar \left(\frac{t_\beta}{2} - t\right) \cdot \left(\frac{t_\beta}{2} + t\right)} \right]. \quad (36)$$

Here,  $t_\alpha = 0$ ,  $(x_\beta - x_\alpha)/2 = L$  as before, and the variable time  $t$  at the slit has been defined to give a symmetric integrand. This integral is derived and evaluated in greater detail in appendix B. The result, given in terms of the complementary error function,  $\text{erfc}(z)$  [25], is

$$I(\beta; \alpha) = \frac{m}{2\pi i \hbar} \pi \cdot \text{erfc}(-i\sqrt{i\varphi_0}) \quad (37)$$

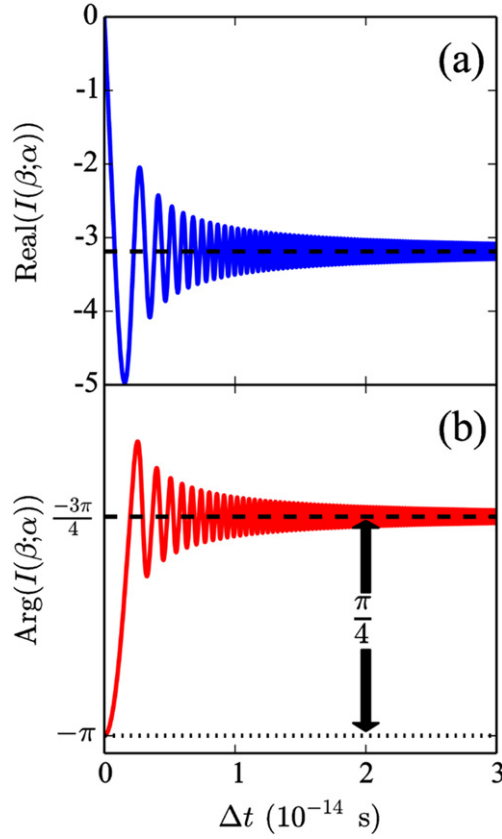


**Figure 4.** Numerical time integration for a single electron path. (a) Real part of (36) (solid blue), integrated from  $-\Delta t/2$  to  $\Delta t/2$  relative to  $t_\beta/2$ , showing convergence to the analytic value given in (37) (dashed line). (b) Complex argument of the integrated amplitude (solid red), showing convergence to  $\pi/4$  phase shift (dashed line) from the argument of  $\exp i\varphi_0$  (dotted black). The amplitude proportional to  $\exp i\varphi_0$  is therefore the appropriate choice of a single amplitude to characterize the entire sum over time.

with  $\varphi_0 \equiv 2mL^2/\hbar t_\beta$ . An asymptotic expansion given by (7.1.23) of [25] gives, for (37),

$$I(\beta; \alpha) \approx \frac{m}{2\pi i \hbar} \sqrt{\frac{\pi}{\varphi_0}} \exp(i\varphi_0) \exp\left(i\frac{\pi}{4} \left[1 - \frac{i}{2\varphi_0} - \frac{3}{4\varphi_0^2} + \frac{15i}{8\varphi_0^3} + \dots\right]\right). \quad (38)$$

The form of (38) illustrates that the total integrated amplitude experiences a phase shift of  $\pi/4$  from the phase  $\varphi_0$ . This phase difference is independent of the choice of path and thus the global phase  $\pi/4$  can be factored out. Figure 4(a) shows the convergence of the real part of the numerical evaluation of (36) (blue curve) to the real part of the analytic result of (37) (black dashed), for  $L = 3.37 \times 10^{-6}$  m and  $t_\beta/2 = 3.36 \times 10^{-13}$  s. The numeric results are computed for variable limits of integration and plotted as a function of the total time interval being integrated. Figure 4(b) gives the phase argument of the numeric results (red curve) to show the convergence of the rotation from the initial phase argument given by  $\varphi_0$ , which is defined by choice of the parameters to be  $-\pi$  (black dotted), to an angle of  $-3\pi/4$  (black dashed). This establishes the appropriate choice of amplitude for a path crossing one slit. The

physical meaning of  $\varphi_0$  will now be discussed. The level of difficulty of this, the previous section, and accompanying appendices A and B is more appropriate for advanced graduate coursework.

## 10. Stationary phase for the two step propagator

The phase  $\varphi$  accumulated along a path crossing a slit is determined from (5) to be

$$\varphi = \frac{m}{2\hbar} \left( \frac{L_1^2}{t_{\text{slit}}} + \frac{L_2^2}{\tau - t_{\text{slit}}} \right), \quad (39)$$

where  $\tau = t_\beta - t_\alpha$ ,  $L_1$  is the path length from source to slit, and  $L_2$  is the length from slit to screen. When  $t_{\text{slit}}$  is varied by  $\delta t_{\text{slit}}$ , the phase can be expanded as a power series in  $\delta t_{\text{slit}}$  as

$$\varphi = \varphi_0 + \frac{\partial \varphi}{\partial t_{\text{slit}}} \delta t_{\text{slit}} + \frac{1}{2} \frac{\partial^2 \varphi}{\partial t_{\text{slit}}^2} (\delta t_{\text{slit}})^2 + \dots, \quad (40)$$

where  $\varphi_0$  is associated with a particular choice of  $t_{\text{slit}}$ . The first-order term of (40) is written out

$$\frac{\partial \varphi}{\partial t_{\text{slit}}} = \frac{m}{2\hbar} \left( \frac{L_2^2}{(\tau - t_{\text{slit}})^2} - \frac{L_1^2}{t_{\text{slit}}^2} \right). \quad (41)$$

The factor  $\partial \varphi / \partial t_{\text{slit}} = 0$  when  $L_2 / (\tau - t_{\text{slit}}) = L_1 / t_{\text{slit}}$ : that is, when the speeds along the path are equal before and after the slit. The phase  $\varphi$  will then experience no first-order variation from  $\varphi_0$  when  $t_{\text{slit}}$  is chosen by this condition. We then say that the phase is stationary for this choice of path, and the value of the stationary phase is  $\varphi_0$ . As shown in section 9, this phase characterizes the amplitude arising from the sum of choosing all values of  $t_{\text{slit}}$ ; therefore, it is the appropriate choice for a single path. The phase in terms of the de Broglie wavelengths along this single path is now established  $\pi L_1 / \lambda_{\text{dB}} + \pi L_2 / \lambda_{\text{dB}} = \pi L_{\text{path}} / \lambda_{\text{dB}}$ . The argument presented here should be appropriate for advanced undergraduates, in what could be a simplified discussion of which paths to choose in the path integral formalism.

## 11. Stationary phase in the double slit

Figure 5(a) shows two interfering paths (green and red) in a space–time diagram for the double slit. The times  $t_{\text{slit}1}$  and  $t_{\text{slit}2}$ , when paths 1 and 2 intersect the slits, respectively, take any value between the initial time  $t_{\text{initial}}$  and final time  $t_{\text{final}}$ . The probability distribution at the screen is shown to the right of the diagram as an intensity plot. In figure 5(b), a phasor diagram of the complex amplitudes for the varying times  $t_{\text{slit}1}$  and  $t_{\text{slit}2}$  is shown. The highlighted paths in figures 5(a) and (b) are the paths of stationary phase. In figure 5(c), the phases corresponding to the amplitudes in (b) are given as a function of time to illustrate the stationary phase behaviour.

Notice that the stationary phase time for path 1, indicated by the largest red dot in figure 5(a), occurs after the stationary phase time for path 2. The reason is that the length of path 1 (that is, the length of the dashed line in the  $x$ – $y$  plane) is shorter than the length of path 2. As the initial time and final times are the same for both paths, the speeds of the paths are different. The equal length of the part of both paths between the source and slits explains the difference in the stationary phase times for this example. For some other path integral

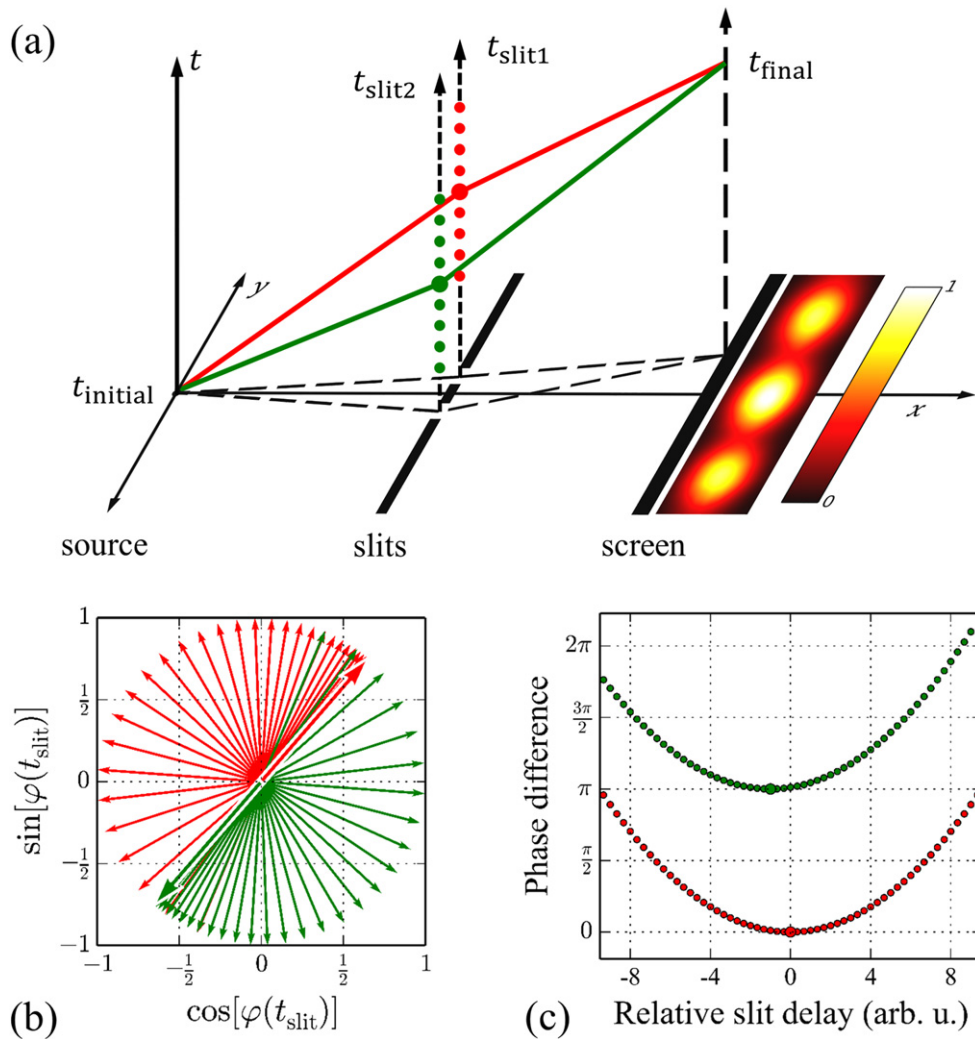


**Figure 5.** Path integral illustration for destructive interference in a double slit. (a) The times  $t_{\text{slit1}}$  and  $t_{\text{slit2}}$  at which the paths intersect the slits take any value between the initial time  $t_{\text{initial}}$  and final time  $t_{\text{final}}$ . The resulting probability distribution at the screen is the square of the sum of the amplitudes for all of the times  $t_{\text{slit1}}$  and  $t_{\text{slit2}}$ . (b) Shown is a phasor diagram for complex amplitudes associated with the intermediate times for slit 1 (red) and slit 2 (green). The highlighted paths in (b) are the paths of stationary phase shown in (a). (c) The phases corresponding to the amplitudes in (b) are shown as a function of intermediate time to illustrate the stationary phase behaviour.

calculations, the slit crossing times are chosen to be identical for all paths [4, 23, 24], while for the optical analogy, the times are the same for paths of the same length from source to slit.

## 12. Phase matters

Does the optical analogy and the path integral method make the same predictions? In other words: ‘does the phase of a single path matter?’ After all, real experiments are only sensitive

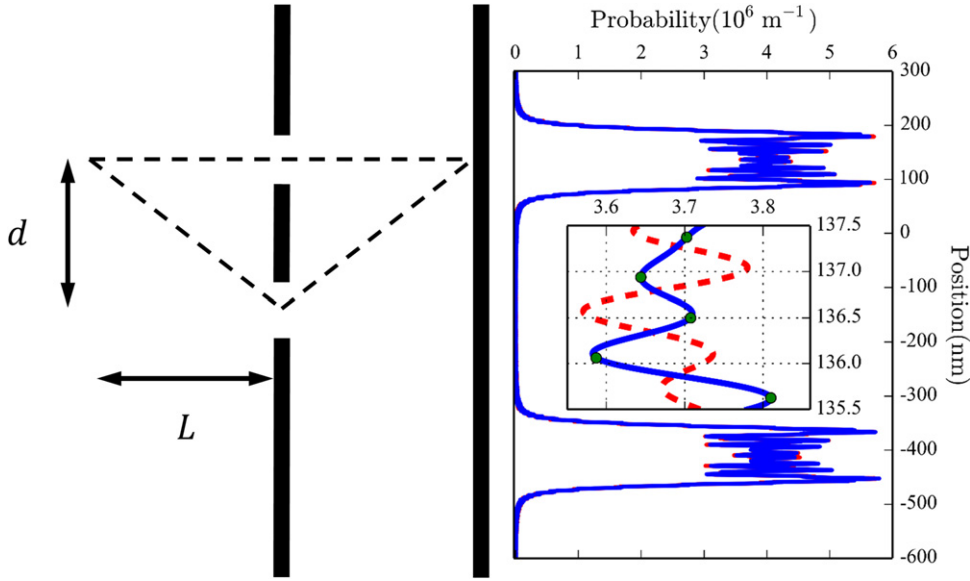


**Figure 6.** Feynman paths and probability distribution from all paths in a near-field two slit arrangement. The source is positioned in line with one of the slits and the detection point. The slit separation  $d$ , propagation length  $L$ , and speed are chosen to highlight the discrepancy between the predictions of the two methods. The normalized probability distribution functions at the screen are computed with the path integral stationary phases (blue), the time-summed amplitudes (green points), and the optical analogy (dashed red).

to phase differences, which were shown to agree for the optical analogy and the path integral formalism in (11). This agreement is not always the case. Consider now the double slit arrangement in figure 6, where the electron source and observation point are in-line with one of the slits. Computing the phases of the drawn paths by (5) (dashed lines) leads to a phase difference

$$\Delta\varphi_{\text{path integral}} = \frac{2md^2}{\hbar\Delta t}. \quad (42)$$

This result does not depend on the length  $L$  in this configuration. If instead we use the optical analogy, we compute the phase difference

$$\Delta\varphi_{\text{optical}} = 2\frac{2\pi}{\lambda_{\text{dB}}(v)} \left( \sqrt{L^2 + d^2} - L \right) \cong \frac{2md^2}{\hbar\Delta t} - \frac{md^4}{2\hbar\Delta tL^2}, \quad (43)$$

where the time and speed between the two methods are connected by  $v = 2L/\Delta t$ . The phase difference in (43) now depends on  $L$ . The phase difference thus depends on the choice of method used for single path phases. When  $d^2/4L^2 \sim \pi\hbar\Delta t/2md^2$ , (43) conflicts with (42), and thus the choice of method matters.

To best exemplify this conflict, let us now choose the experimental conditions so that the common term of (42) and (43) is set to an integer multiple of  $2\pi$ , and the second term of (43) set to  $\pi$ . Now, (42) predicts constructive interference in line with the slit, while (43) predicts destructive interference. For electron diffraction in the symmetric double slit arrangement of figure 6, a slit separation of 273 nm with widths of 63 nm can be chosen. Note that such a

double slit has been demonstrated recently for electron diffraction in [4]. In contrast to [4], now the source and screen are placed at the much closer distances of  $3.37 \mu\text{m}$  from the slits. When  $\Delta t$  is fixed for the path integral method by choosing the electron speed to be  $10^7 \text{ m s}^{-1}$  over the straight path, the difference of  $\pi$  is set between the predictions of the two methods. The diffraction patterns are computed with both methods and shown on the right of figure 6. At a location on the detection screen that is in line with the source (at  $y = 136.5 \text{ nm}$ ), the path integral method (solid blue) predicts a constructive maximum, while the optical analogy (dashed red) predicts a minimum. A time sum of the form of (35) performed for 6000 points per slit and five points on the observation screen over intervals of  $6.88 \times 10^{-14} \text{ s}$  centred on the stationary phase time of each path from the source to the screen points (green points) agrees with the blue curve computed with the stationary phase times alone. This configuration is experimentally challenging to realize. Nevertheless, near field interferometry for matter waves does exist and may be pushed towards this regime [26, 27]. In conclusion, phase difference predictions from the optical analogy and the path integral formalism will not agree in some near-field conditions. While the global phase of a single path does not matter, to obtain correct phase differences, the single path phases must be handled appropriately. This result, which follows from the stationary phase argument of section 10, could be presented in an advanced undergraduate course, but the technical details of justifying the stationary path results for the simulation would again be a topic for an advanced graduate course.

### 13. Summary and conclusions

The optical analogy can give excellent approximate phase differences in most situations and thus leads to the correct prediction of the positions of interference extrema. This method is justified by considering stationary solutions to the Schrödinger equation. The conceptual trap is that a student may infer from the correct phase difference,  $2\pi\Delta L/\lambda$ , that the phase of a single path is given by  $2\pi L/\lambda$  (as would be correct for optical waves). The path integral description of quantum mechanics gives the correct phase difference  $2\pi\Delta L/\lambda$  between paths, the correct phase  $\pi L/\lambda$  accumulated over time along a single path, and justifies drawing ‘paths’ in space to compute phases. The path integral method (and the time-dependent Schrödinger equation) gives the exact phase difference in all situations. It is therefore an appropriate method to use in conceptual discussions of matter wave diffraction.

In some physics textbooks, both paths and waves are omitted from the description of matter wave diffraction. Instead, the discussion refers back to water waves or Young’s experiment for light waves and quotes the condition for interference or phase differences by analogy [28–32]. This presentation is correct to obtain phase differences, but it ignores the differences in propagation, that is, the time dependent behaviour, between light and matter waves.

Some physics textbooks [30–32], as well as some advanced undergraduate and graduate texts, will draw attention to group and phase velocities in sections unrelated to the double slit description [15, 33, 34]. It is interesting to contemplate at what level and in what manner the conceptual difficulty discussed in this paper could be addressed. For example, it could follow a discussion of the group and phase velocities of a matter wave packet. The results from the path integral formalism could thus be presented at the undergraduate level [35–37] to elucidate the idea of a ‘path’.

## Acknowledgments

The authors gratefully acknowledge discussions with Ron Capelletti, Sam Werner, Mike Snow, Bradley Shadwick, Ilya Fabrikant, and Mathieu Beau. ERJ, RAB, and HB gratefully acknowledge funding from the NSF (grant numbers 0969506 and 1306565). ERJ also gratefully acknowledges funding from the DOE GAANN programme number 58558.

## Appendix A. Time sum derivation

In the following, the propagator is derived for a single slit crossing as described in section 9. In (31), each of the positions  $x_k$  represent the range of positions a point could have along a path at the  $k$ th time step of the sum. Requiring that a path intersects the slit at  $x_{\text{slit}}$  in the  $k$ th time step is defined as a multiplication of a term  $\delta(x_{\text{slit}} - x_k)$  to the integrand. This intersection happens at any time step from the first up to the last, so a factor

$$\chi_{\text{slit}} = \sum_{k=1}^{N-1} \delta(x_{\text{slit}} - x_k) \quad (\text{A.1})$$

must be included in (31) to describe all of the alternative times a path can intersect the slit. Substituting (A.1) into (31) gives the total amplitude to travel from  $\alpha$  to  $\beta$  as

$$\begin{aligned} K(\beta; \alpha) &= \lim_{\epsilon \rightarrow 0} \left( \frac{m}{2\pi i \hbar \epsilon} \right)^{N/2} \int \dots \int \chi_{\text{slit}} \exp \left[ \frac{im}{2\hbar \epsilon} \sum_{j=1}^N (x_j - x_{j-1})^2 \right] dx_1 \dots dx_{N-1} \\ &= \lim_{\epsilon \rightarrow 0} \sum_{k=1}^{N-1} \left( \frac{m}{2\pi i \hbar \epsilon} \right)^{N/2} \int \dots \int \exp \left[ \frac{im}{2\hbar \epsilon} \sum_{j=1}^N (x_j - x_{j-1})^2 \right] \\ &\quad \times \delta(x_{\text{slit}} - x_k) dx_1 \dots dx_{N-1}. \end{aligned} \quad (\text{A.2})$$

Performing the  $N - 1$  integrations in (A.2) leads to the total sum

$$K(\beta; \alpha) = \lim_{\epsilon \rightarrow 0} \sum_{k=1}^{N-1} K(x_\beta, t_\beta; x_{\text{slit}}, t_\alpha + k\epsilon) \cdot K(x_{\text{slit}}, t_\alpha + k\epsilon; x_\alpha, t_\alpha). \quad (\text{A.3})$$

The substitution  $t_{\text{slit}} \equiv t_\alpha + k\epsilon$  is made into (A.3) to obtain the final result

$$\begin{aligned} K(\beta; \alpha) &= \lim_{\epsilon \rightarrow 0} \sum_{t_{\text{slit}}=t_\alpha+\epsilon}^{t_\beta-\epsilon} K(x_\beta, t_\beta; x_{\text{slit}}, t_{\text{slit}}) \cdot K(x_{\text{slit}}, t_{\text{slit}}; x_\alpha, t_\alpha) \\ &= \sum_{t_{\text{slit}}=t_\alpha}^{t_\beta} K(x_\beta, t_\beta; x_{\text{slit}}, t_{\text{slit}}) \cdot K(x_{\text{slit}}, t_{\text{slit}}; x_\alpha, t_\alpha). \end{aligned} \quad (\text{A.4})$$

## Appendix B. Evaluating the integral of the full time sum

The time sum derived in (A.4) over the continuous value  $t_{\text{slit}}$  must be handled carefully near the singular points occurring at  $t_{\text{slit}} = t_\beta$  and  $t_{\text{slit}} = t_\alpha = 0$ , so we convert the sum to an integral prior to performing the limit  $\epsilon \rightarrow 0$  to obtain

$$I(\beta; \alpha) = \lim_{\epsilon \rightarrow 0} \int_{\epsilon}^{t_{\beta} - \epsilon} dt_{\text{slit}} \frac{m}{2\pi i \hbar} \left[ \frac{1}{t_{\text{slit}}(t_{\beta} - t_{\text{slit}})} \right]^{1/2} \exp \left[ \frac{imL^2 \cdot t_{\beta}}{2\hbar t_{\text{slit}}(t_{\beta} - t_{\text{slit}})} \right], \quad (\text{B.1})$$

where  $(x_{\beta} - x_{\alpha})/2 = L$  as before. Next,  $x = 2(t_{\text{slit}}/t_{\beta} - 1/2)$  is substituted to obtain

$$I(\beta; \alpha) = \lim_{\epsilon \rightarrow 0} \int_{-1 + \frac{2\epsilon}{t_{\beta}}}^{1 - \frac{2\epsilon}{t_{\beta}}} dx \frac{m}{2\pi i \hbar} \left[ \frac{1}{(1+x)(1-x)} \right]^{1/2} \exp \left[ \frac{i2mL^2}{\hbar t_{\beta}} \frac{1}{(1+x)(1-x)} \right]. \quad (\text{B.2})$$

Equation (B.2) is simplified by the definition of the stationary phase as  $\varphi_0 \equiv 2mL^2/\hbar t_{\beta}$  as in section 9. The next substitution to be performed is  $x = \sin(\theta)$ . This trigonometric substitution eliminates the square root, as  $dx/\sqrt{1-x^2} = d\theta$ , and we obtain

$$\begin{aligned} I(\beta; \alpha) &= \lim_{\epsilon \rightarrow 0} \frac{m}{2\pi i \hbar} \int_{\sin^{-1}\left(-1 + \frac{2\epsilon}{t_{\beta}}\right)}^{\sin^{-1}\left(1 - \frac{2\epsilon}{t_{\beta}}\right)} d\theta \exp \left( \frac{i\varphi_0}{\cos^2(\theta)} \right) \\ &= \lim_{\epsilon \rightarrow 0} \frac{m}{2\pi i \hbar} \int_{\sin^{-1}\left(-1 + \frac{2\epsilon}{t_{\beta}}\right)}^{\sin^{-1}\left(1 - \frac{2\epsilon}{t_{\beta}}\right)} d\theta \exp(i\varphi_0) \cdot \exp \left( i\varphi_0 \tan^2(\theta) \right), \end{aligned} \quad (\text{B.3})$$

where the identity  $\sec^2(\theta) = 1 + \tan^2(\theta)$  is used in order to factor out a term  $\exp i\varphi_0$ . Next, we substitute  $u = \tan(\theta)$  and obtain

$$I(\beta; \alpha) = \lim_{\epsilon \rightarrow 0} \frac{m}{2\pi i \hbar} \exp(i\varphi_0) \int_{\tan\left[\sin^{-1}\left(-1 + \frac{2\epsilon}{t_{\beta}}\right)\right]}^{\tan\left[\sin^{-1}\left(1 - \frac{2\epsilon}{t_{\beta}}\right)\right]} du \frac{\exp(i\varphi_0 u^2)}{1 + u^2}. \quad (\text{B.4})$$

The limits of integration are symmetric and now tend to  $\pm\infty$  as  $\epsilon \rightarrow 0$ , so they are redefined as  $\tan\left[\sin^{-1}\left(1 - 2\epsilon/t_{\beta}\right)\right] = R$  and  $\tan\left[\sin^{-1}\left(-1 + 2\epsilon/t_{\beta}\right)\right] = -R$ , with the limit  $R \rightarrow \infty$ . Finally, we extend the integrand into the complex plane by performing the substitution  $t = -i\sqrt{i\varphi_0}u$  to obtain

$$I(\beta; \alpha) = \lim_{R \rightarrow \infty} \frac{m}{2\pi i \hbar} \exp(i\varphi_0) i\sqrt{i\varphi_0} \int_{-i\sqrt{i\varphi_0}(-R)}^{-i\sqrt{i\varphi_0}R} dt \frac{\exp(-t^2)}{\left(\sqrt{i\varphi_0}\right)^2 - t^2}. \quad (\text{B.5})$$

The integrand is analytic everywhere in the complex plane except for first-order poles at  $\pm\sqrt{i\varphi_0}$ , therefore the path of integration, which lies on the line  $t = R \exp(i3\pi/4)$ , can be rotated to lie entirely on the real axis. The integrand's even symmetry then permits

$$I(\beta; \alpha) = \frac{m}{2i\hbar} \exp(i\varphi_0) \left[ \frac{2i}{\pi} \sqrt{i\varphi_0} \int_0^{\infty} dt \frac{\exp(-t^2)}{\left(\sqrt{i\varphi_0}\right)^2 - t^2} \right]. \quad (\text{B.6})$$

The term in square brackets of (B.6) has the form of the complex-valued function  $w(z)$ , given in (7.1.4) of [25], as

$$w(z) = \frac{2iz}{\pi} \int_0^{\infty} dt \frac{\exp(-t^2)}{z^2 - t^2}. \quad (\text{B.7})$$

This function can be readily evaluated from the definitions given in (7.1.2) and (7.1.3) of [25], as

$$w(z) = \exp(-z^2) \operatorname{erfc}(-iz), \quad (\text{B.8})$$

where  $\operatorname{erfc}(z)$  is the complementary error function. Substituting (B.7) and (B.8) into (B.6), we obtain the result,

$$I(\beta; \alpha) = \frac{m}{2\pi i \hbar} \pi \cdot \operatorname{erfc}\left(-i\sqrt{i\varphi_0}\right), \quad (\text{B.9})$$

which is (37).

## References

- [1] Young T 1804 The bakerian lecture: experiments and calculations relative to physical optics *Phil. Trans. R. Soc. A* **94** 1–16
- [2] Young T 1807 *A Course of Lectures on Natural Philosophy and the Mechanical Arts* vol 1 (London: William Savage) pp 464–8, 776–7, 786–7
- [3] Feynman R P, Leighton R B and Sands M L 1965 *The Feynman Lectures on Physics* vol 3 (Reading, MA: Addison-Wesley) pp 1–6
- [4] Bach R, Pope D, Liou S Y and Batelaan H 2013 Controlled double-slit electron diffraction *New J. Phys.* **15** 033018
- [5] Feynman R P 1948 Space–time approach to non-relativistic quantum mechanics *Rev. Mod. Phys.* **20** 367–87
- [6] Schrödinger E 1982 *Collected Papers on Wave Mechanics* 3rd edn (New York: Chelsea) pp 102–4
- [7] Dirac P A M 1945 On the analogy between classical and quantum mechanics *Rev. Mod. Phys.* **17** 195–9
- [8] Feynman R P and Hibbs A R 2005 *Quantum Mechanics and Path Integrals* emended edn ed D F Styer (Mineola, NY: Dover) pp 26–47
- [9] Cronin A D, Schmiedmayer J and Pritchard D E 2009 Optics and interferometry with atoms and molecules *Rev. Mod. Phys.* **81** 1051–129
- [10] Sabra A I 1981 *Theories of Light from Descartes to Newton* (New York: Cambridge University Press) pp 136–58
- [11] Feynman R P 2006 *QED: the strange theory of light and matter* (Princeton, NJ: Princeton University Press) pp 36–76
- [12] Born M and Wolf E 1993 *Principles of Optics* 6th edn (Tarrytown, NY: Pergamon) pp 109–32
- [13] Landau L D and Lifshitz E M 1975 *The Classical Theory of Fields* 4th edn (Burlington, MA: Elsevier) pp 140–3
- [14] Adams C S, Sigel M and Mlynek J 1994 *At. Opt. Phys. Rep.* **240** 143–210
- [15] Griffiths D J 2005 *Introduction to Quantum Mechanics* 2nd edn (Upper Saddle River, NJ: Pearson Prentice Hall) pp 59–67
- [16] Bohm D 1989 *Quantum Theory* (Mineola, NY: Dover) pp 59–66
- [17] Jackson J D 1999 *Classical Electrodynamics* 3rd edn (Hoboken, NJ: Wiley) pp 478–82
- [18] Moshinsky M 1952 Diffraction in time *Phys. Rev.* **88** 625–31
- [19] Brukner Č and Zeilinger A 1997 Diffraction of matter waves in space and time *Phys. Rev. A* **56** 3804–24
- [20] Beau M and Dorlas T C 2014 Three-dimensional quantum slit diffraction and diffraction in time *Int. J. Theor. Phys.* **54** 1882–907
- [21] Szriftgiser P, Guéry-Odelin D, Andt M and Dalibard J 1996 Atomic wave diffraction and interference using temporal slits *Phys. Rev. Lett.* **77** 4–7
- [22] Hils Th F J, Gähler R, Gläser W, Golub R, Habicht K and Wille P 1998 Matter-wave optics in the time domain: results of a cold-neutron experiment *Phys. Rev. A* **58** 4784–90
- [23] Barut A O and Basri S 1992 Path integrals and quantum interference *Am. J. Phys.* **60** 896–9
- [24] Beau M 2012 Feynman path integral approach to electron diffraction for one and two slits: analytical results *Eur. J. Phys.* **33** 1023–39
- [25] Abramowitz M and Stegun I A 1965 *Handbook of Mathematical Functions with Formulas, Graphs, and Mathematical Tables* 9th edn (Mineola, NY: Dover) pp 297–8
- [26] McMorran B J and Cronin A D 2009 An electron talbot interferometer *New J. Phys.* **11** 033021
- [27] Bach R, Gronniger G and Batelaan H 2013 A charged particle Talbot-Lau interferometer and magnetic field sensing *Appl. Phys. Lett.* **103** 254102

- [28] Giancoli D C 2013 *Physics: Principles with Applications* 7th edn (New York: Pearson Education, Inc.) pp 682–5, 805–6
- [29] Walker J S 2002 *Physics* (Upper Saddle River, NJ: Prentice-Hall) pp 916–20, 995–1001
- [30] Young H D and Freedman R A 2012 *Sears and Zemansky's University Physics: with Modern Physics* 13th edn (San Francisco, CA: Addison-Wesley) pp 1163–73, 1314–5
- [31] Krane K S 2012 *Modern Physics* 3rd edn (Hoboken, NJ: Wiley) pp 72–3, 107–10
- [32] Ohanian H C 1995 *Modern Physics* 2nd edn (Upper Saddle River, NY: Prentice-Hall) p 21, pp 144–50
- [33] Cohen-Tannoudji C, Diu B and Laloë F 2005 *Quantum Mechanics* vol 1 2nd edn (New York: Wiley) pp 21–31, 61–6
- [34] Liboff R L 2003 *Introductory Quantum Mechanics* 4th edn (San Francisco, CA: Addison-Wesley) pp 46–7, 82–4, 156–7
- [35] Cohen S M 1998 Path integral for the quantum harmonic oscillator using elementary methods *Am. J. Phys.* **66** 537–40
- [36] Taylor E F, Vokos S, O'Meara J M and Thornber N S 1998 Teaching Feynman's sum-over-paths quantum theory *Comput. Phys.* **12** 190–9
- [37] Malgieri M, Onorato P and De Ambrosio A 2014 Teaching quantum physics by the sum over paths approach and GeoGebra simulations *Eur. J. Phys.* **35** 055024